Journal of Statistical Physics, Vol. 44, Nos. 5/6, 1986

Dimer Pair Correlations on the Brick Lattice

Carlos S. O. Yokoi,[1,3] John F. Nagle,[1] and Silvio R. Salinas[2]

Received March 3, 1986

Using exact methods, pair-correlation functions are studied in the dimer model defined on a brick lattice. At long distances these functions exhibit strongly anisotropic algebraic decay and, near criticality, the length scales diverge differently in the two principal directions. The critical exponents are $\nu_x = \frac{1}{2}$ and $\nu_y = 1$. These results are in agreement with deductions drawn from recent exact finite-size scaling calculations. We also interpret our results in the light of domain wall theories of commensurate–incommensurate transitions, and in particular we study the relation of the present model to the discrete version of the Pokrovsky–Talapov model introduced by Villain.

KEY WORDS: Dimers, K_i-models, pair correlations, phase transitions, commensurate–incommensurate transition, domain walls.

1. INTRODUCTION

Some interesting properties of the dimer model on the brick (or honeycomb) lattice (see Fig. 1) were first pointed out by Kasteleyn[1] who solved the partition function problem exactly. His solution showed that the system remains "frozen" in a state identical to the ground state for temperatures below the critical temperature at which it undergoes a phase transition to the disordered phase. The source of this intriguing result can be traced back to the dimer constraints imposed by the brick lattice which force the number of horizontal dimers in the rows to be a conserved quantity. As a consequence there is an infinite energy gap between the ground state and the first excited states, which accounts for the peculiar behavior.

[1] Department of Physics, Carnegie-Mellon University, Pittsburgh, Pennsylvania 15213.
[2] Instituto de Fisica, Universidade de Sao Paulo, C. P. 20.516, Sao Paulo, Brazil.
[3] Permanent Address: Instituto de Fisica, Universidade de Sao Paulo, C. P. 20.516, Sao Paulo, Brazil.

0022-4715/86/0900-0729$05.00/0

822/44/5-6-2

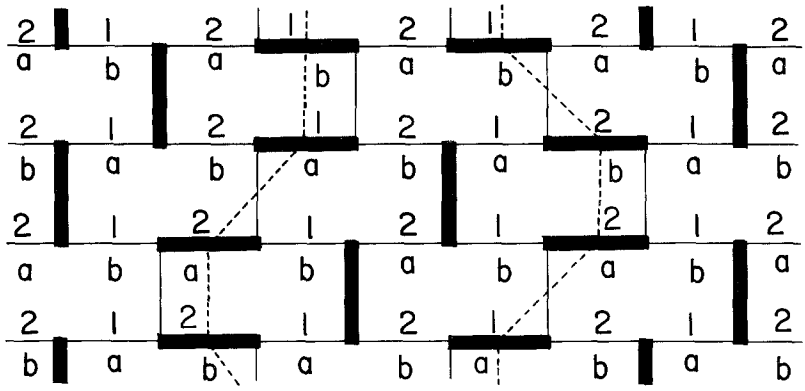

Fig. 1. One of many states of the K-model. The brick lattice is represented by light solid lines and the heavy lines represent dimers, each of which covers one bond and two lattice sites. In the K-model each horizontal dimer costs an energy ε, whereas vertical dimers cost no energy. In the K_2-model solved in this paper, each dimer on a horizontal bond labeled 1 or 2 costs an energy ε_1 or ε_2, respectively. In the original K_1-model solved by Kasteleyn, each dimer on a horizontal bond labeled a or b costs an energy ε_a or ε_b, respectively. The configuration of dimers in the figure corresponds to a domain wall state consisting of two walls, indicated by dashed lines.

The rather unusual characteristics of this model, which has been called the Kasteleyn model or simply the K-model,[2] have been applied advantageously to study a number of different physical systems including polymers,[3] lipid bilayer biomembranes,[2,4] and ferroelectrics.[5,6] Of more immediate interest to us in the present work is the recent recognition of the fact that the K-model is also an exactly solvable model of domain walls[7,8] and as such is relevant to the study of commensurate–incommensurate (CI) transitions of monolayers adsorbed on rectangular substrates.[9]

The main objective of this paper is to study the dimer–dimer correlation functions in the K-model. The long-distance behavior of these correlation functions provides a test of the general phenomenological theory of domain walls,[10] which predicts the existence of distinct diverging length scales in the two orthogonal directions with critical exponents $\nu_x = \frac{1}{2}$ and $\nu_y = 1$. The results confirm the conclusion of a recent exact finite-size scaling analysis of the K-model,[11] which gave strong, but indirect, evidence for the existence of these diverging length scales. Another of our objectives is to study a possible connection of the K-model to a particular domain wall model of CI transitions introduced by Villain.[2] In the next section we introduce a new variation of the K-model which is most suitable for this comparison. We will name this the K_2-model. We compute the partition function and the dimer densities for this model and in the third sec-

tion we calculate dimer–dimer correlation functions. The asymptotic form of the correlation functions allows us to identify the critical exponents associated with the two diverging length scales. Finally, in the last section we present one possible way to map the K_2-model to the Villain model.[12] The mapping is only approximate, but we argue that under suitable conditions the approximation involved is justified, which permits the application of the results derived for the K_2-model to the Villain model.

2. PARTITION FUNCTION AND DIMER DENSITIES

Let us consider the statistical mechanics of the brick lattice fully packed with dimers such that each lattice site is occupied by one and only one dimer, as shown in Fig. 1. In this work we consider a particular variant of the K-model, to be called the K_2-model, for which the dimers on the vertical bonds have zero energy and those on the horizontal bonds of alternating columns have energies $\varepsilon_1 > 0$ and $\varepsilon_2 > 0$, respectively. The original model studied by Kasteleyn,[1] which might be called the K_1-model, also has three energies; 0, ε_a, and ε_b, but the assignment of energies to the bonds obeys a hexagonal symmetry rather than the rectangular symmetry of the K_2-model. In the cases when $\varepsilon_1 = \varepsilon_2 = \varepsilon$ and $\varepsilon_a = \varepsilon_b = \varepsilon$, both models reduce to the same model, which is the one usually called the K-model.[2,7,8,11] The motivation behind defining the new K_2-model will be clarified in Section 4, where we relate it to the Villain model of domain walls.

The partition function for the K_2-model is defined as

$$Z = \sum_{\text{states}} z_1^{N_1} z_2^{N_2} \tag{1}$$

where $z_i = \exp(-\beta\varepsilon_i)$, for $i = 1, 2$ with $\beta = 1/k_B T$, are the activities and N_i is the number of dimers on the i-type horizontal bonds. According to the general theorems due to Kasteleyn,[1,13] the partition function of the dimer problem on any planar lattice (with free boundaries) can be expressed as a Pfaffian of a suitably constructed antisymmetric matrix A: $Z = \mathrm{Pf}(A) = [\det(A)]^{1/2}$. The bond orientations and the unit cell for the construction of the matrix A are shown in Fig. 2. For a lattice with N_x and N_y cells in the horizontal and vertical directions, respectively, the partition function in the bulk limit $N_x, N_y \to \infty$ is given by[13]

$$\frac{1}{N_x N_y} \ln Z = \frac{1}{2(2\pi)^2} \int_0^{2\pi} \int_0^{2\pi} d\phi_1 \, d\phi_2 \ln \det \Lambda(\phi_1, \phi_2) \tag{2}$$

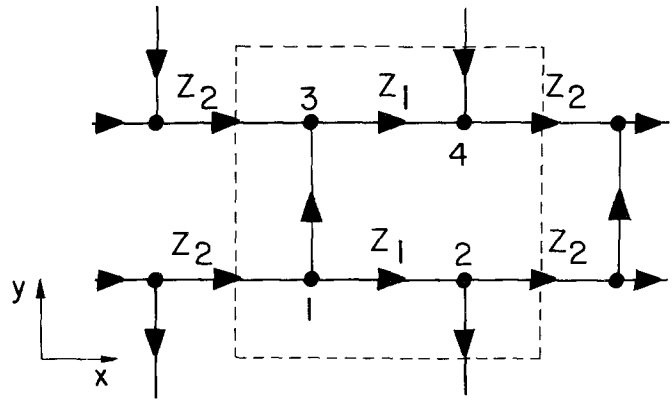

Fig. 2. The dashed lines indicated the unit cell and the arrows show the bond orientations for the application of the Pfaffian method. The activities of horizontal bonds are labeled z_1 and z_2 and the activities of the vertical bonds are equal to 1.

where $\Lambda(\phi_1, \phi_2)$ is a 4×4 matrix with the following nonzero elements

$$\begin{aligned} \Lambda_{12} &= \Lambda_{34} = -\Lambda_{21}^* = -\Lambda_{43}^* = z_1 - z_2 e^{i\phi_1} \\ \Lambda_{13} &= -\Lambda_{31}^* = 1 \\ \Lambda_{24} &= -\Lambda_{42}^* = e^{i\phi_2} \end{aligned} \tag{3}$$

The determinant of the matrix $\Lambda(\phi_1, \phi_2)$ is found to be

$$\det \Lambda(\phi_1, \phi_2) = | \, |z_1 - z_2 e^{i\phi_1}|^2 - e^{i\phi_2}|^2 \tag{4}$$

The nature of the low- and the high-temperature phases can be deduced from the densities of different types of dimers in these phases. The density of i-type horizontal dimers is given by

$$\rho_i = \frac{\langle N_i \rangle}{N} = \frac{z_i}{2} \frac{\partial}{\partial z_i} \frac{\ln Z}{N_x N_y} \tag{5}$$

where $N = 2N_x N_y$ is the total number of dimers. For example, the expression for the 1-type horizontal dimers is

$$\rho_1 = \frac{z_1}{(2\pi)^2} \int_0^{2\pi} d\phi_1 (z_1 - z_2 \cos \phi_1) \int_0^{2\pi} d\phi_2 \frac{|z_1 - z_2 e^{i\phi_1}|^2 - \cos \phi_2}{\det \Lambda(\phi_1, \phi_2)} \tag{6}$$

Using contour integration, the double integral can be computed in closed

form.[4] In expressing the results it is helpful to introduce the angular variable ϕ_0 defined as

$$\phi_0 = \sin^{-1}\left[\frac{(z_1+z_2)^2-1}{4z_1z_2}\right]^{1/2} \qquad \text{if} \quad z_1+z_2>1 \tag{7}$$

and $\phi_0 = 0$ if $z_1+z_2 \leqslant 1$. In terms of the variable ϕ_0, the density of horizontal 1-type dimers can be written in the form

$$\rho_1 = \frac{\phi_0}{\pi} + \text{sign}(z_1-z_2)\left[\frac{1}{2} - \frac{1}{\pi}\tan^{-1}\left(\frac{z_1+z_2}{|z_1-z_2|}\cot\phi_0\right)\right] \tag{8}$$

We observe that ρ_1 vanishes for $z_1+z_2 \leqslant 1$. Since the partition function is symmetric in the activities z_1 and z_2, it follows that $\rho_2(z_1, z_2) = \rho_1(z_2, z_1)$. Also, the density of dimers on the vertical bonds is $\rho_v = 1-\rho_1-\rho_2$, given by the simple expression

$$\rho_v = 1 - \frac{2}{\pi}\phi_0 \tag{9}$$

The preceding results show that the model exhibits a phase transition at a critical temperature T_c determined by the equation

$$z_{1c}+z_{2c} = \exp\left(-\frac{\varepsilon_1}{k_B T_c}\right) + \exp\left(-\frac{\varepsilon_2}{k_B T_c}\right) = 1 \tag{10}$$

From eq. 9 it follows that below T_c the density of vertical dimers is unity, that is, the low-temperature phase is a fully ordered state with all dimers lying on the vertical bonds. The critical properties of various thermodynamic quantities as one approaches the transition point are governed essentially by the variable ϕ_0. Equation 7 gives for $t \equiv (T-T_c)/T_c \to 0+$ the asymptotic result

$$\phi_0 = \left[\frac{1}{2k_B T_c}\left(\frac{\varepsilon_1}{z_{2c}} + \frac{\varepsilon_2}{z_{1c}}\right)\right]^{1/2} t^{1/2} + O(t^{3/2}) \tag{11}$$

Using Eq. 11 we conclude that the dimer densities behave as $\rho_1 \approx t^{1/2}$, $\rho_2 \approx t^{1/2}$, and $1-\rho_v \approx t^{1/2}$ when $t \to 0+$. The internal energy per dimer is given by $u = \varepsilon_1\rho_1 + \varepsilon_2\rho_2$, so that it also behaves as $u \approx t^{1/2}$ when $t \to 0+$. It then follows that the specific heat per dimer, $c = du/dT$, has the asymptotic behavior $c \approx t^{-1/2}$ as $t \to 0+$ while it is zero below T_c, which implies that the values of the critical exponents are $\alpha' = 0$ and $\alpha = \frac{1}{2}$. Thus the K_2-model belongs to the class of models exhibiting the "3/2-order transition."[14]

3. DIMER–DIMER CORRELATION FUNCTIONS

Fisher and Stephenson[15] developed a general perturbation theory of Pfaffians in order to study the correlation properties of the dimer model on the square lattice. The method can be generalized to other planar lattices[16] along the lines of the work of Montroll, Potts, and Ward who studied the correlation functions of the Ising model by transforming it into a dimer problem.[17] In this section we are interested in the correlations between pairs of dimers in the deep interior of an infinite brick lattice. The pair-correlation function between the bonds a and b is defined as[15]

$$C_{ab} = P_{ab} - P_a P_b \tag{12}$$

where P_a and P_b denote the occupation probabilities of the bonds a and b, and P_{ab} is the joint occupation probability of the bonds a and b. According to the perturbation theory of Pfaffians,[15] the quantity C_{ab} can be expressed in terms of the basic antisymmetric matrix $\mathrm{A} = (\mathrm{A}_{ij})$ in the form

$$C_{ab} = -A_{ij} A_{kl} (G_{ik} G_{jl} - G_{il} G_{jk}) \tag{13}$$

where the bonds are denoted by their endpoints, $a = (i, j)$, and $b = (k, l)$, and $\mathrm{G} = (\mathrm{G}_{ij}) = \mathrm{A}^{-1}$ is the Green's function matrix. The explicit expression for the Green's function elements in the deep interior of an infinite lattice is[16,17]

$$\begin{aligned} G_{jk} &= [x' - x,\ y' - y]_{\alpha\alpha'} \\ &= \frac{1}{(2\pi)^2} \int_0^{2\pi} \int_0^{2\pi} d\phi_1\, d\phi_2\, \Lambda^{-1}_{\alpha\alpha'}(\phi_1, \phi_2)\, e^{-i(x'-x)\phi_1 - i(y'-y)\phi_2} \end{aligned} \tag{14}$$

where (x, y) and (x', y') denote the coordinates of the lattice cell containing the points j and k, respectively, and the numbers α and α' are the identifying numbers of these points inside the unit cells in Fig. 2. The nonzero elements of the inverse matrix $\Lambda^{-1}(\phi_1, \phi_2)$ are

$$\begin{aligned} \Lambda^{-1}_{12} &= -\Lambda^{-1*}_{21} = \frac{-z_1 + z_2 e^{i\phi_1}}{|z_1 - z_2 e^{i\phi_1}|^2 - e^{i\phi_2}} \\ \Lambda^{-1}_{13} &= -\Lambda^{-1*}_{31} = \frac{e^{i\phi_2}}{|z_1 - z_2 e^{i\phi_1}|^2 - e^{i\phi_2}} \\ \Lambda^{-1}_{24} &= -\Lambda^{-1*}_{42} = \frac{1}{|z_1 - z_2 e^{i\phi_1}|^2 - e^{-i\phi_2}} \\ \Lambda^{-1}_{34} &= -\Lambda^{-1*}_{43} = \frac{-z_1 + z_2 e^{i\phi_1}}{|z_1 - z_2 e^{i\phi_1}|^2 - e^{-i\phi_2}} \end{aligned} \tag{15}$$

From the integral expression for the Green's function elements eq. 14 and using eqs. 15 we find the following identities

$$\begin{aligned}
&[x, y]_{\alpha\beta} = -[-x, -y]^*_{\beta\alpha} = -[-x, -y]_{\beta\alpha} \\
&[x, y]_{14} = [x, y]_{23} = [x, y]_{\alpha\alpha} = 0 \\
&[x, y]_{13} = [x, -y-1]_{24} \\
&[x, y]_{12} = [x, -y]_{34} \\
&[x, y]_{34} = -z_1[x, y]_{24} + z_2[x+1, y]_{24}
\end{aligned} \tag{16}$$

Equations 16 show that all the Green's function elements are related in a simple way to the element $[x, y]_{24}$. From Eqs. 14 and 15 we have, explicitly

$$[x, y]_{24} = \frac{1}{(2\pi)^2} \int_0^{2\pi} \int_0^{2\pi} d\phi_1 \, d\phi_2 \, \frac{e^{-ix\phi_1 - iy\phi_2}}{|z_1 - z_2 e^{i\phi_1}|^2 - e^{-i\phi_2}} \tag{17}$$

By carrying out the integration over ϕ_2 we obtain, for $y \geqslant 0$

$$[x, y]_{24} = \frac{2}{\pi}(-1)^x \int_0^{\phi_0} d\phi \, \frac{\cos 2x\phi}{|z_1 + z_2 e^{2i\phi}|^{2(y+1)}} \tag{18}$$

and, for $y < 0$

$$[x, y]_{24} = -\frac{2}{\pi}(-1)^x \int_{\phi_0}^{\pi/2} d\phi \, \frac{\cos 2x\phi}{|z_1 + z_2 e^{2i\phi}|^{2(y+1)}} \tag{19}$$

where ϕ_0 was defined in Eq. 7. We observe in passing that for $y = -1 (x \neq 0)$ we get from Eq. 19 the particularly simple result

$$[x, -1]_{24} = (-1)^x \frac{\sin 2\phi_0 x}{\pi x} \tag{20}$$

In order to characterize the different dimer-pair correlations, it is convenient to denote the six primitive bonds, two vertical and four horizontal, by the letters v, v', h_1, h_2, h_1', and h_2', as shown in Fig. 3. As an example we consider the pair-correlation function between two vertical v dimers. Using Eq. 13 we have

$$C_{vv}(x, y) = -([x, y]_{11}[x, y]_{33} - [x, y]_{13}[x, y]_{31}) \tag{21}$$

With the help of the identities in Eqs. 16 we can put Eq. 21 in the form involving only the elements $[x, y]_{24}$

$$C_{vv}(x, y) = -[x, -y-1]_{24}[-x, y-1]_{24} \tag{22}$$

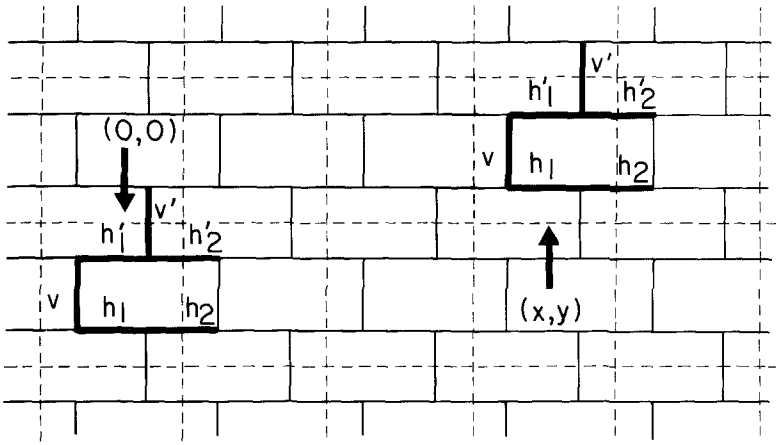

Fig. 3. The notations for the primitive bonds of the unit cells employed in the calculation of the dimer–dimer correlation functions. The two-unit cells indicated by arrows and by labeled bonds are separated by $(x, y) = (3, 1)$.

We observe that for the case of vertical v dimers in the same row, $y = 0$ and $x \neq 0$, the application of Eq. 20 gives a particularly simple and *exact* expression

$$C_{vv}(x, 0) = -\frac{\sin^2(2\phi_0 x)}{\pi^2 x^2} \tag{23}$$

In order to get an intuitive feeling for the spread of short-range dimer correlations, we give in Table I the numerical values of the pair correlations between the horizontal 1-type bond shown in the bottom left corner of Table I and the neighboring bonds. We considered the case $z_1 = z_2$ and reduced temperature $t = 0.1$. The numbers in Table I are pair correlations multiplied by 10^6. The densities, or single-occupation probabilities of the vertical and horizontal dimers, can be computed using eqs. 8 and 9. In the present case they are $\rho_v = 0.77636427...$ and $\rho_1 = \rho_2 = \rho_h = 0.11181786...$. For the two horizontal bonds adjoining the given h_1 bond as well as for the given h_1 bond itself we find for the correlations the value $-\rho_h^2 = -0.01250323...$. For the two vertical bonds adjoining the given h_1 bond the correlation is $-\rho_v \rho_h = -0.08681139...$. For these bonds, therefore, the joint occupation probability is zero, which simply reflects the fact that two dimers cannot overlap at the same site. Also, the sum of the correlations of the three bonds incident to one of the two sites occupied by the given dimer is just $-\rho_h$. Furthermore, the sum of the correlations of any three bonds that meet at a common site not occupied by the given

Table I. Numerical Values of the Dimer-Correlation Function ($\times 10^6$) Relative to the Horizontal Bond in the Bottom Left Corner (indicated by asterisk) for the Case $z_1 = z_2$ and $t = 0.1$[a]

	−10966		**56**		**5607**		**2508**		**35**		**477**
6916	**7611**	**3354**	**3048**	−3104	−2262	−3345	−1686	−823	−41	**6**	−78	−399
	−14527		−6402		**5366**		**5030**		**864**		**72**	
7263	**7263**	**7263**	−861	−709	−4657	−2952	−2078	−731	−133	**72**	−144	−378
	−14527			**1570**		**7609**		**2809**		**61**		**521**
9803	**10755**	**3772**	**3438**	−5008	−3694	−3915	−2053	−756	−90	**29**	−126	−395
	−20558		−7210		**8703**		**5968**		**846**		**97**	
10279	**10279**	**10279**	−3068	−2542	−6160	−3987	−1981	−763	−83	**29**	−126	−411
	−20558			**5611**		**10147**		**2744**		**54**		**537**
15899	**17388**	**3169**	**2897**	−8508	−6350	−3797	−2066	−678	−122	**68**	−158	−379
	−33287		−6067		**14858**		**5863**		**800**		**90**	
16643	**16643**	**16643**	−10577	−8822	−6036	−3984	−1879	−781	−19	**4**	−93	−431
	−33287			**19399**		**10020**		**2661**		**15**		**524**
41527	**45284**	−11997	−11002	−8397	−6339	−3681	−2072	−588	−138	**123**	−174	−351
	−86811		**22999**		**14735**		**5754**		**726**		**50**	
−12503	−12503*	−12503	−10496	−8811	−5924	−3983	−1771	−788	**61**	−5	−46	−437
	−86811			**19307**		**9907**		**2559**		**56**		**483**

[a] Positive correlations have been printed in boldface. This table is similar to a figure given by Fisher and Stephenson[15] for dimers on a square lattice except that they normalized the correlation function to be −1 on the horizontal bond in the bottom-left corner.

dimer is zero; this reflects the obvious requirement that precisely one of the three bonds is always occupied by a dimer.

Table I gives a picture of the effect of the presence of an horizontal dimer on the occupation probabilities of the neighboring bonds. It is clear that the presence of a horizontal dimer enhances the occupation probabilities of the horizontal bonds along the y direction and depresses most of the occupation probabilities of the horizontal bonds along the x direction. The opposite can be said about the occupation probabilities of the vertical bonds. However, there is also a nearly vertical line of horizontal bonds located approximately 4.5 unit cells away from the given horizontal dimer where the occupation probabilities are enhanced. These observations find a natural explanation if we consider the dimer configurations that occur above the critical temperature. As has been pointed out by many authors,[1,2,7] the dimer constraints in this model impose a conservation of the number of horizontal dimers in each horizontal row. As a result, the horizontal dimers form stripes, or domain walls, running along the y direc-

tion, as can be seen in Fig. 1. The average density of these walls ρ_w should obey the equation

$$\rho_w = \frac{\langle N_1 + N_2 \rangle}{2N_x N_y} \tag{24}$$

where the factor 2 accounts for the existence of two horizontal bonds in each unit cell. The average distance between the walls l is then given by

$$\frac{1}{l} = \rho_w = \left\langle \frac{N_1 + N_2}{N} \right\rangle = \rho_1 + \rho_2 = 1 - \rho_v = \frac{2}{\pi}\phi_0 \tag{25}$$

At the particular temperature under consideration we find $l = 4.471557...$, which is consistent with the distance seen in Table I for the vertical line of horizontal bonds where the occcupation probabilities are enhanced. The oscillatory nature of the correlation functions between pairs of vertical dimers along the x direction, given by eq. 23, can also be interpreted as resulting from the presence of these walls. In fact, eq. 23 shows local maxima at intervals $\pi/2\phi_0$, which is precisely the average separation between the walls.

Let us now consider the long-range dimer correlation functions, which are of principal interest in the study of critical phenomena. First we derive the asymptotic expressions for Green's function elements. We consider the situation $T > T_c$ and $(x^2 + y^2)^{1/2} \to \infty$ with fixed ratio $x/y = \text{const.}$ Introducing the polar coordinates $x = r\cos\theta$, $y = r\sin\theta$ and the function

$$h(\phi) = -\sin\theta \ln(z_1^2 + z_2^2 + 2z_1 z_2 \cos 2\phi) + i2\phi\cos\theta \tag{26}$$

we can rewrite Green's function element $[x, y]_{24}$ for $y \geqslant 0$ in the form

$$[x, y]_{24} = \frac{2}{\pi}(-1)^x \operatorname{Re} \int_0^{\phi_0} dz \frac{\exp[rh(z)]}{z_1^2 + z_2^2 + 2z_1 z_2 \cos 2z} \tag{27}$$

and for $y < 0$ as

$$[x, y]_{24} = -\frac{2}{\pi}(-1)^x \operatorname{Re} \int_{\phi_0}^{\pi/2} dz \frac{\exp[rh(z)]}{z_1^2 + z_2^2 + 2z_1 z_2 \cos 2z} \tag{28}$$

For both integrals the real part of the function $h(z)$ is maximum at the endpoint $z = \phi_0$ so that we apply the steepest descent method[18] to the vicinity of this endpoint to determine the asymptotic expression for $r \to \infty$. The final result, independent of the sign of y, is

$$[x, y]_{24} \sim \frac{(-1)^x}{\pi\xi_x} \frac{(x/\xi_x)\sin(x/\xi_x) + (y/\xi_y)\cos(x/\xi_x)}{(x/\xi_x)^2 + (y/\xi_y)^2} \tag{29}$$

where

$$\xi_x = \frac{1}{2\phi_0} \tag{30}$$

and

$$\xi_y = \frac{1}{4z_1 z_2 \phi_0 \sin 2\phi_0} \tag{31}$$

Using eq. 22 and the asymptotic result eq. 29, we obtain the following asymptotic expresion for dimer-pair correlations between two vertical bonds

$$C_{vv}(x, y) \sim -\frac{1}{\pi^2 \xi_x^2} \frac{(x/\xi_x)^2 \sin^2(x/\xi_x) - (y/\xi_y)^2 \cos^2(x/\xi_x)}{[(x/\xi_x)^2 + (y/\xi_y)^2]^2}$$
$$\equiv C(x, y) \tag{32}$$

valid for $t \to 0+$ and $\sqrt{x^2+y^2} \to \infty$. In the asymptotic regime all the dimer–dimer correlation functions are proportional to $C(x, y)$, defined in eq. 32, according to

$$C_{ab}(x, y) \sim K_{ab} C(x, y) \tag{33}$$

where the proportionality factors K_{ab} are given in Table II for all possible bond combinations.

The quantities ξ_x and ξ_y defined in eqs. 30 and 31 set the length scales in eq. 32 for the decay of the correlation functions in the two orthogonal directions. Therefore, they find a natural interpretation as the *correlation*

Table II. The Coefficients K_{ab}[a]

	v	v'	h_1	h_2	h'_1	h'_2
v	1	$(z_1+z_2)^2$	$-z_1(z_1+z_2)$	$-z_2(z_1+z_2)$	$-z_1(z_1+z_2)$	$-z_2(z_1+z_2)$
v'	$(z_1+z_2)^2$	1	$-z_1(z_1+z_2)$	$-z_2(z_1+z_2)$	$-z_1(z_1+z_2)$	$-z_2(z_1+z_2)$
h_1	$-z_1(z_1+z_2)$	$-z_1(z_1+z_2)$	$z_1^2(z_1+z_2)^2$	$z_1 z_2(z_1+z_2)^2$	z_1^2	$z_1 z_2$
h_2	$-z_2(z_1+z_2)$	$-z_2(z_1+z_2)$	$z_1 z_2(z_1+z_2)^2$	$z_2^2(z_1+z_2)^2$	$z_1 z_2$	z_2^2
h'_1	$-z_1(z_1+z_2)$	$-z_1(z_1+z_2)$	z_1^2	$z_1 z_2$	$z_1^2(z_1+z_2)^2$	$z_1 z_2(z_1+z_2)^2$
h'_2	$-z_2(z_1+z_2)$	$-z_2(z_1+z_2)$	$z_1 z_2$	z_2^2	$z_1 z_2(z_1+z_2)^2$	$z_2^2(z_1+z_2)^2$

[a] As defined in eq. 33, giving the asymptotic formulas for all possible dimer–dimer correlation functions. These coefficients are symmetric with respect to the permutation of indices, $K_{ab} = K_{ba}$ due to the symmetry requirement $C_{ab}(x, y) = C_{ba}(-x, -y)$, which can be deduced from Eq. 13 and the identities Eq. 16.

lengths in the model. Since, from eq. 11, $\phi_0 \approx t^{1/2}$ for $t \to 0+$, it follows from eqs. 30 and 31 that the correlation lengths diverge as the critical points is approached from above as

$$\xi_x \approx t^{-\nu_x}, \qquad \xi_y \approx t^{-\nu_y} \tag{34}$$

with $\nu_x = \frac{1}{2}$ and $\nu_y = 1$. These values of the critical exponents ν_x and ν_y are in complete agreement with general phenomenological theories of domain walls.[10] They also confirm the conclusions of a recent finite-size calculation of the K-model[11]; that study, however, did not provide a direct proof of the existence of these correlation lengths in the infinite lattice.

It is also revealing to rewrite the asymptotic, i.e., scaling, formula, for the correlation functions in terms of scaled distances X and Y defined by

$$X = \frac{x}{\xi_x} \qquad \text{and} \qquad Y = \frac{y}{\xi_y} \tag{35}$$

which are then reexpressed in terms of polar coordinates

$$R^2 = X^2 + Y^2 \qquad \text{and} \qquad \Theta = \cos^{-1}(X/R) \tag{36}$$

Then the function $C(x, y)$ defined in eq. 32 becomes

$$C(R, \Theta) = -\frac{1}{\pi^2 \xi_x^2} \frac{\sin(\Theta + R\cos\Theta)\sin(\Theta - R\cos\Theta)}{R^2} \tag{37}$$

Equation 37 emphasizes the qualitatively different behavior for $\Theta = 0$, for which the correlations oscillate in sign, from the behavior for $\Theta = \pi/2$, for which the decay is monotonic. It also emphasizes that the scaling function undergoes a smooth transformation from one behavior to the other as a function of Θ with the wavelength of the oscillations scaling as $1/\cos\Theta$. Another way to see the highly anisotropic nature of the model is provided in Fig. 4 in which the zeros of the asymptotic correlation function and the regions of positive and negative correlation functions are shown. The loci of zeros is given by the simple formula $Y = \pm X \tan X$, as can be checked from eq. 32 or 37.

The preceding results have straightforward meanings in terms of the domain wall picture described before. The negative correlations seen in Fig. 4 can be interpreted as arising from the repulsive nature of the walls.[8,19] The positive long-range dimer correlations running along the y direction at $x = 0$ is consistent with the existence of the wall at the origin running preferentially along the y direction, which tends to enhance the joint occupation probabilities along this direction. The other regions of

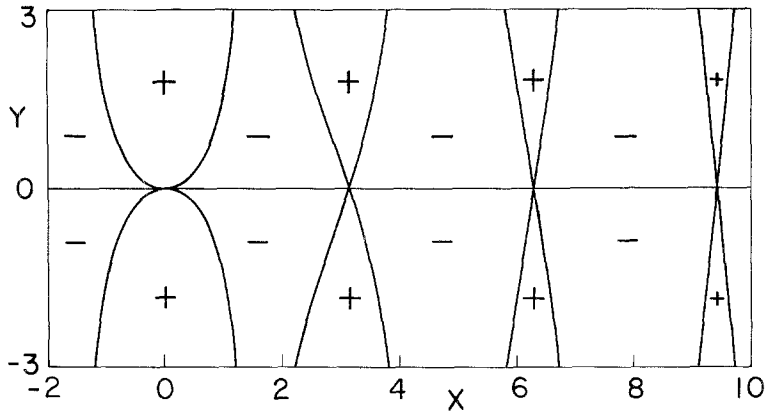

Fig. 4. Zeros of the asymptotic scaling correlation function given by eq. 37. The X and Y axes are the dimensionless scaled lengths given by eq. 35. The solid curves show the loci of the zeros and the signs indicate the regions where the correlations are positive and negative, respectively.

positive correlations correspond to the other walls running in parallel. This intrinsic anisotropy of the wall model is clearly connected to the two distinct *correlation lengths* given by eqs. 30 and 31.

The temperature plays two roles in determining the correlation functions in eq. 37. The first is in determining the scaled distances, eq. 35, through the correlation lengths as already described in eq. 34. In addition, there is an explicit factor proportional to $\xi_x^{-2} \approx t = (T - T_c)/T_c$ in eq. 37. The necessity of this t factor will now be illustrated. First, we recall that the specific heat of the model C_V is related to the dimer–dimer correlation functions, C_{ab}, through the formula

$$C_V = \frac{1}{kT^2} \sum_{ab} \varepsilon_a \varepsilon_b C_{ab} \tag{38}$$

where ε_a and ε_b are the energies of the bonds a and b, respectively, and the sum extends over all pair of bonds in the lattice. (The unsolved problem of defining an independent susceptibility and of finding those correlations which, when summed, give the undefined susceptibility, has been discussed for the K-model[2].) Therefore, the leading singular part of the specific heat behaves as

$$C_V \approx \iint C(x, y)\, dx\, dy \approx t\xi_x \xi_y \iint t^{-1} C(X, Y)\, dX\, dY \tag{39}$$

Since the integrand of the last integral does not depend upon temperature,

the entire asymptotic temperature dependence comes from the three prefactors which, by eq. 34, yield the known result that $C_V \approx t^{-1/2}$.

Finally, let us observe that the dimer correlations decay algebraically with distance as $r^{-\eta}$, with $\eta = 2$, as can be seen from eq. 37. This result was already established by Sutherland[20]; from that paper the result $\xi_x \approx (T - T_c)^{-1/2}$ can also be obtained, but the ξ_y correlation length and the anisotropy of the correlations are not evident. The dimer correlations on the square lattice also exhibit algebraic decay.[1,15] However, algebraic decay of the correlations is not a necessary feature of all dimer models, as can be seen from the dimer model on the 4–8 lattice where the decay of dimer correlations is exponential.[16] In the case of the K-model the algebraic decay may be attributed to the fact that the walls formed by horizontal dimers are never allowed to break or go backward. If such defects or *dislocations* are allowed, as in the recently proposed dimer model with dislocations,[21] we expect exponential decay typical of the fluid phase.

4. RELATIONSHIP TO THE VILLAIN MODEL OF DOMAIN WALLS

The main purpose of this last section is to show that the K_2-model can be mapped *approximately* to the Villain model,[12] which is a discrete version of the two-dimensional Pokrovsky–Talapov model of the domain walls.[22] The recent interest in two-dimensional domain wall models originates from the study of CI transitions often observed in monolayers of adsorbed atoms or molecules.[9] In the commensurate phase the adsorbed monolayer forms an ordered structure commensurate with the underlaying lattice. As the temperature or chemical potential is varied, the commensurate phase may undergo a phase transition into a disordered, fluid phase, into another commensurate phase, or into an incommensurate phase. According to current ideas, the transition from commensurate to incommensurate phase occurs through the spontaneous creation of domain walls or misfit lines, which separate regions of essentially commensurate order. The simplest systems that have been considered are those with uniaxial, rectangular symmetry. The commensurate phase is then a $p \times 1$ uniaxial phase, where the absorbate atoms form a superlattice in which the lattice constant along one direction is p times larger than the corresponding substrate lattice constant. Such commensurate phases have been observed, for example, in hydrogen adsorbed on Fe(110).[23] The statistical mechanics of the $p \times 1$ uniaxial models has been studied by many authors using different techniques.[19,22,24,25,26]

The Villain model,[12] defined on a square lattice of size $N_x \times N_y$, is a discrete model of walls with hard-core repulsion between them. The walls

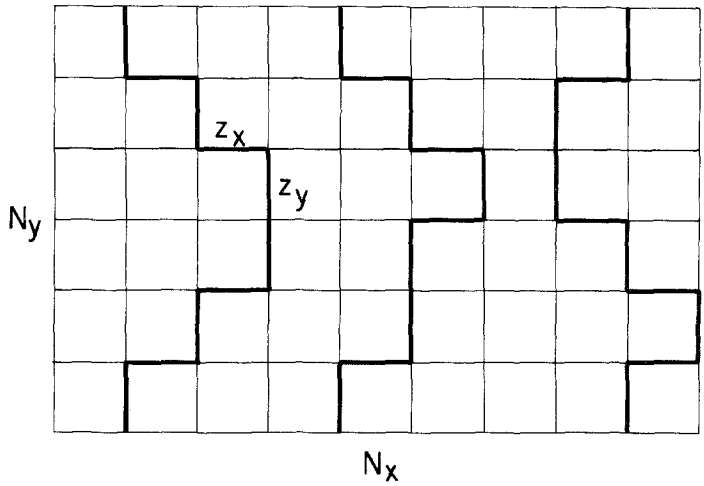

Fig. 5. Villain model of domain walls. The bold lines represent the domain walls lying on a square lattice of size $N_x \times N_y$. z_x and z_y represent the activities associated with horizontal and vertical bonds, respectively. The walls cannot turn backward or cross each other, and no two consecutive horizontal wall segments are allowed.

are represented by lines formed by horizontal and vertical bonds, as shown in Fig. 5, with the constraint that no segment of the wall can be formed by two consecutive horizontal bonds. These walls are also constrained to transverse the whole lattice from top to bottom without turning backward and they are forbidden from crossing each other.[12] This model should then be appropriate for the description of the 1×1 CI transition in the absence of *dislocations*. To the portion of walls lying on vertical bonds we attribute the activity

$$z_y = \exp(-\beta\mu^*) \tag{40}$$

where μ^* is the *effective chemical potential* of the walls.[12] On the other hand, to the portion of walls lying on the horizontal bonds we attribute the activity

$$z_x = \exp(-\beta\gamma) \tag{41}$$

where γ is the *line tension* of the walls.[12] The grand canonical partition function for the system of walls is

$$\Xi = \sum_{\text{allowed configuations}} z_x^{n_x} z_y^{n_y} \tag{42}$$

where n_x and n_y denote the number of horizontal and vertical bonds belonging to the walls.

In order to relate the Villain model to the K_2-model we superimpose the square lattice of the Villain model on the square lattice formed by the unit cells of the K_2-model, as shown in Fig. 6. For each 2-type horizontal dimer we associate half of a vertical bond of the wall, whereas to the 1-type horizontal dimer we associate one horizontal bond in addition to half of a vertical bond of the wall. This correspondence implies the following relationship between the dimer activities and the wall activities:

$$\begin{aligned} z_2 &= z_y^{1/2} = \exp(-\beta\mu^*/2) \\ z_1 &= z_x z_y^{1/2} = \exp(-\beta\gamma - \beta\mu^*/2) \end{aligned} \tag{43}$$

To each wall configuration in the Villain model there is a corresponding dimer configuration in the K_2-model with the same energy, but the converse is not always true. In fact, some dimer configurations correspond to wall configurations that are not included in the Villain model. One typical case is illustrated in Fig. 6. However, for a sufficiently high line tension, $\beta\gamma \gg 1$, these extra configurations only make an insignificant contribution

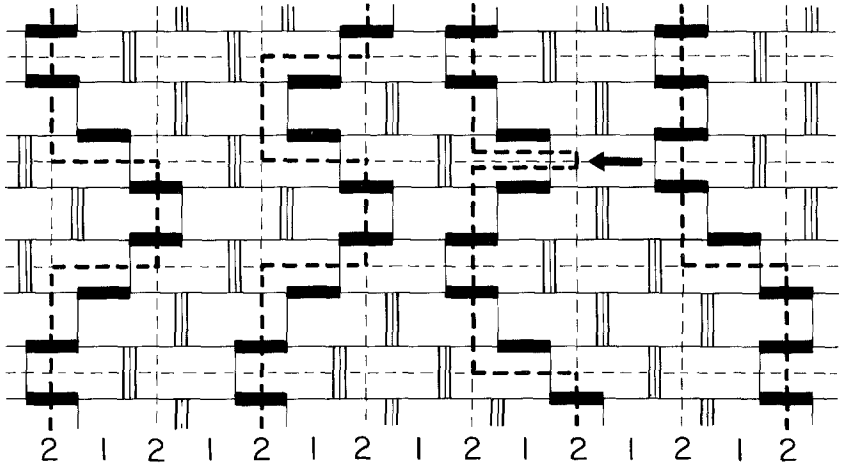

Fig. 6. The mapping of the K-model to the Villain model. The brick lattice is shown in light solid lines. Vertical dimers are represented by open vertical rectangles on the brick latice and horizontal dimers are represented by solid rectangles. The numbers $i = 1, 2$ at the bottom of the figure indicate that those horizontal dimers located directly above a number i have activities z_i, similar to Fig. 1. The square lattice of the Villain model is coincident with the superlattice of unit cells represented by dashed lines. The walls in the Villain model are represented by heavy dashed lines. Every state of the Villain model corresponds to a dimer configuration, but not all dimer configurations correspond to an allowed state of the Villain model. The dimer configuration indicated by the arrow shows one instance where there is no corresponding Villain configuration.

to the partition function. Therefore, under this restriction we have the following *approximate* equality of the partition function of the dimer model and the grand canonical partition function of the Villain model

$$Z(z_1, z_2) \approx \Xi(z_x, z_y) \tag{44}$$

We remark that the transfer matrix approach used by Villain[12] based on the "free fermion approximation" also involves a similar degree of approximation. Therefore, we expect the two methods to give the same values of thermodynamic functions only if $\beta\gamma \gg 1$. Otherwise they must give different results for nonuniversal quantities, but we argue that the critical exponents should still be expected to be the same.

We can now translate the results of the previous sections on the K_2-model to the case of the Villain model. The phase transition is determined by eq. 10, which becomes in this case

$$z_1 + z_2 = e^{-\beta\mu^*/2}(1 + e^{-\beta\gamma}) = 1 \tag{45}$$

Since we assume $\beta\gamma \gg 1$, the above expression can be approximated by

$$\beta\mu^* = 2e^{-\beta\gamma} \tag{46}$$

which is identical to eq. IV-4 of Ref. (12).

The degree of incommensurability of an incommensurate phase is given by the density of walls or *incommensurability* $\bar{q}$. The average distance between the walls has been calculated before and is given by eq. 25. Therefore, the incommensurability in the Villain model is given by

$$\bar{q} = \frac{1}{l} = \frac{2}{\pi}\phi_0 \tag{47}$$

From eq. 11 we obtain for $\beta\gamma \gg 1$ and $t \to 0+$ the result

$$\phi_0 \sim \left(\frac{1 + \beta_c\gamma}{2}\right)^{1/2} t^{1/2} \tag{48}$$

Substituting eq. 48 into eq. 47 we obtain

$$\frac{\pi}{l} \sim \sqrt{2(1 + \beta_c\gamma)}\, t^{1/2} \tag{49}$$

in agreement with eq. VI-5 of Ref. (12). The square root dependence of the incommensurability near the CI transition in two dimensions, $\bar{q} \approx t^{\bar{\beta}}$ where $\bar{\beta} = \frac{1}{2}$, was first obtained by Pokrovsky and Talapov.[22]

We can define the wall–wall correlation function in the same manner as the dimer–dimer correlation function defined in eq. 12, where now P_a, P_b, and P_{ab} represent, respectively, the single and joint occupation probabilities of the bonds a and b by the walls. Since the presence or absence of the walls correspond to the presence or absence of horizontal dimers of type h_2 and h'_2, we can identify the wall–wall correlations $C_{ww}(x, y)$ to the dimer–dimer correlations $C_{h_2h_2}(x, y)$, $C_{h_2h'_2}(x, y)$, $C_{h'_2h_2}(x, y)$, or $C_{h'_2h'_2}(x, y)$. In the asymptotic regime $t \to 0+$ and $\sqrt{x^2+y^2} \to \infty$, all these dimer–dimer correlations give the same result, and we have

$$C_{ww}(x, y) \sim -\frac{1}{\pi^2 \xi_x^2} \frac{(x/\xi_x)^2 \sin^2(x/\xi_x) - (y/\xi_y)^2 \cos^2(x/\xi_x)}{[(x/\xi_x)^2 + (y/\xi_y)^2]^2} \tag{50}$$

where the *characteristic lengths* are given by

$$\xi_x = \frac{1}{2\phi_0} \sim [2(1+\beta_c\gamma)]^{-1/2} t^{-1/2} \tag{51}$$

and

$$\xi_y = \frac{1}{4z_1 z_2 \phi_0 \sin 2\phi_0} \sim \frac{e^{\beta_c \gamma}}{4(1+\beta_c\gamma)} t^{-1} \tag{52}$$

In order to avoid any false impressions we stress the fact that the results of this section are approximate only to the extent that the K_2-model was applied to the solution of a different lattice model problem which can be related to the K_2-model only approximately. It is then important to emphasize that the K_2-model with the identification of the domain walls given in Fig. 1 is in itself a *bona fide* exactly solvable domain wall model.[7,8,11] We also mention that a dimer model with dislocations that has the K-model as a limiting case has been discovered and studied by exact methods.[21] Together with the results of the present paper, it can be concluded that the K-model and its variations constitute a well-defined exactly solvable class of discrete lattice models having anisotropic, domain wall, commensurate–incommensurate transitions that provide rigorous tests of more general, but less exact, theories.

ACKNOWLEDGMENT

We wish to acknowledge, in decreasing order of financial support for this research, the Brazilian agencies CNPq, FAPESP, and United States NSF Grant DMR 8115979.

REFEENCES

1. P. W. Kasteleyn, *J. Math. Phys.* **4**:287 (1963).
2. J. F. Nagle, *Phys. Rev. Lett.* **34**:1150 (1975).
3. J. F. Nagle, *Proc. Roy. Soc. Lond. A* **337**:569 (1974).
4. J. F. Nagle, *J. Chem. Phys.* **58**:252 (1973).
5. J. F. Nagle and G. R. Allen, *J. Chem. Phys.* **55**:2708 (1971).
6. F. Y. Wu, *Phys. Rev.* **168**:539 (1968).
7. S. M. Bhattacharjee, J. F. Nagle, D. A. Huse, and M. E. Fisher, *J. Stat. Phys.* **32**:361 (1983).
8. M. E. Fisher, *J. Stat. Phys.* **34**:667 (1984).
9. P. Bak, *Rep. Prog. Phys.* **45**:587 (1982).
10. D. A. Huse and M. E. Fisher, *Phys. Rev. B* **29**:239 (1984).
11. S. M. Bhattacharjee and J. F. Nagle, *Phys. Rev. B* **31**:3199 (1985).
12. J. Villain, in *Ordering in Strongly Fluctuating Condensed Matter Systems*, T. Riste, ed. (Plenum, New York, 1980).
13. E. W. Montroll, in *Applied Combinatorial Mathematics*, E. F. Beckenbach, ed. (Wiley, New York, 1964).
14. J. F. Nagle, *Proc. Nat. Acad. Sci. U.S.A.* **70**:3443 (1973).
15. M. E. Fisher and J. Stephenson, *Phys. Rev.* **132**:1411 (1963).
16. S. R. Salinas and J. F. Nagle, *Phys. Rev. B* **9**:4920 (1974).
17. E. W. Montroll, R. B. Potts, and J. C. Ward, *J. Math. Phys.* **4**:308 (1963).
18. N. G. de Bruijn, in *Asymptotic Methods in Analysis*, chap. 5 (Dover, New York, 1981).
19. M. E. Fisher and D. S. Fisher, *Phys. Rev. B* **25**:3192 (1982).
20. B. Sutherland, *Phys. Lett. A* **26**:532 (1968).
21. S. M. Bhattacharjee, *Phys. Rev. Letts.* **53**:1161 (1984).
22. V. L. Pokrovsky and A. L. Talapov, *Phys. Rev. Letts.* **42**:65 (1979).
23. R. Imbihl, R. J. Behm, K. Christmann, G. Ertl, and T. Matsushima, *Surf. Sci.* **117**:257 (1982).
24. H. J. Schultz, *Phys. Rev. B* **22**:5274 (1980).
25. H. J. Schultz, *Phys. Rev. B* **28**:2746 (1983).
26. F. D. Haldane, P. Bak, and T. Bohr, *Phys. Rev. B* **28**:2743 (1983).